

4-1-2004

# Determination of the optical dispersion in ferroelectric vinylidene fluoride (70%)/trifluoroethylene (30%) copolymer Langmuir-Blodgett films

Mengjun Bai

*University of Nebraska-Lincoln*, baime@missouri.edu

A.V. Sorokin

*University of Nebraska - Lincoln*

Daniel W. Thompson

*University of Nebraska - Lincoln*

Matt Poulsen

*University of Nebraska-Lincoln*, map@suiiter.com

Stephen Ducharme

*University of Nebraska*, sducharme1@unl.edu

*See next page for additional authors*

Follow this and additional works at: <http://digitalcommons.unl.edu/physicsducharme>

 Part of the [Physics Commons](#)

---

Bai, Mengjun; Sorokin, A.V.; Thompson, Daniel W.; Poulsen, Matt; Ducharme, Stephen; Herzinger, C.M.; Palto, S.; Fridkin, V.M.; Yudin, S.G.; Savchenko, V.E.; and Gribova, L.K., "Determination of the optical dispersion in ferroelectric vinylidene fluoride (70%)/trifluoroethylene (30%) copolymer Langmuir-Blodgett films" (2004). *Stephen Ducharme Publications*. 6.  
<http://digitalcommons.unl.edu/physicsducharme/6>

This Article is brought to you for free and open access by the Research Papers in Physics and Astronomy at DigitalCommons@University of Nebraska - Lincoln. It has been accepted for inclusion in Stephen Ducharme Publications by an authorized administrator of DigitalCommons@University of Nebraska - Lincoln.

---

**Authors**

Mengjun Bai, A.V. Sorokin, Daniel W. Thompson, Matt Poulsen, Stephen Ducharme, C.M. Herzinger, S. Palto, V.M. Fridkin, S.G. Yudin, V.E. Savchenko, and L.K. Gribova

# Determination of the optical dispersion in ferroelectric vinylidene fluoride (70%)/trifluoroethylene (30%) copolymer Langmuir–Blodgett films

Mengjun Bai and A. V. Sorokin<sup>a)</sup>

*Department of Physics and Astronomy, Center for Materials Research and Analysis, University of Nebraska, Lincoln, Nebraska 68588-0111*

Daniel W. Thompson

*Department of Electrical Engineering, Center for Materials Research and Analysis, University of Nebraska, Lincoln, Nebraska 68588-0111*

Matt Poulsen and Stephen Ducharme<sup>b)</sup>

*Department of Physics and Astronomy, Center for Materials Research and Analysis, University of Nebraska, Lincoln, Nebraska 68588-0111*

C. M. Herzinger

*J. A. Woollam Company, 645 M St. Lincoln, Nebraska 68508*

S. Palto, V. M. Fridkin, and S. G. Yudin

*Institute of Crystallography, Russian Academy of Sciences, Leninsky Prospect 59, Moscow 117333, Russia*

V. E. Savchenko and L. K. Gribova

*State Institute for Machinery Research and Development (NIEKMI), 39 Suvorov St., Ivanovo 153012, Russia*

(Received 4 August 2003; accepted 18 December 2003)

We report measurements of the optical dispersion in ferroelectric Langmuir–Blodgett films of polyvinylidene fluoride (70%)-trifluoroethylene (30%) copolymer, using variable-angle spectroscopic ellipsometry over a wide spectral range from infrared to ultraviolet. Film thickness averaged  $1.78 \pm 0.07$  nm per deposition layer for films ranging from 5 to 125 deposition layers as determined from multi-sample analysis. This deposition rate was consistent with capacitance measurements, yielding a dielectric constant of  $9.9 \pm 0.4$  normal to the film, by quartz microbalance measurements, and by atomic force microscopy. © 2004 American Institute of Physics.

[DOI: 10.1063/1.1649464]

## I. INTRODUCTION

Polyvinylidene fluoride (PVDF), and its copolymers with trifluoroethylene [P(VDF/TrFE)], are widely used as audio frequency and ultrasonic acoustic transducers, as electro-mechanical actuators, and as heat detectors, because of their piezoelectric and pyroelectric properties.<sup>1,2</sup> These materials also have good nonlinear optical properties in a wide spectral range,<sup>3</sup> potentially useful for frequency conversion and fiber optical sensors.<sup>4</sup> Moreover, the built-in electrical polarization also makes it possible to modulate the optical properties by applying an external electrical field.<sup>5</sup> The optical properties of PVDF<sup>3,5,6</sup> and the PVDF/TrFE copolymers have been studied experimentally<sup>7–9</sup> and theoretically.<sup>10–12</sup> Films prepared by solution processing methods usually exhibit large optical scattering due to the inhomogeneous structure of lamellar crystals embedded in an amorphous matrix.<sup>13</sup> The highly oriented films<sup>8</sup> and extended-chain samples<sup>9,14</sup> have higher crystallinity and more uniform crystal orientation. The films made by the LB method are polycrystalline with chains parallel to the film, as revealed by x-ray diffraction<sup>15,16</sup> and polarized infrared spectra,<sup>17</sup> and seem to be without lamellar

structure. Previous reports give the optical refractive indices at only one or two wavelengths, and for partially oriented samples. In this work, we report the measurements of the optical dispersion in PVDF/TrFE copolymer LB films in the wide spectral range from infrared (IR) to ultraviolet (UV) by using variable-angle spectroscopic ellipsometry (VASE).

VASE is a useful tool for characterization of material optical properties, especially for thin films.<sup>18</sup> The optical properties of a material can be expressed by the complex tensor  $\tilde{n}(\lambda) = n(\lambda) + ik(\lambda)$ , where  $n(\lambda)$  and  $k(\lambda)$  are the refractive index and attenuation constant tensors, respectively, and  $\lambda$  is the wavelength. In the VASE reflection mode, the incident and reflected polarization states are measured, yielding the complex ratio  $\rho(\lambda, \theta) = \tan[\psi(\lambda, \theta)] \exp[i\Delta(\lambda, \theta)] = r_s(\lambda, \theta)/r_p(\lambda, \theta)$ , where  $\tan \psi$  is the reflectance ratio,  $\Delta$  is the retardance, and  $r_s$  and  $r_p$  are the complex Fresnel reflection coefficients. The subscripts “s” and “p” refer to the polarization component perpendicular and parallel to the plane of incidence, respectively. The optical constants  $n(\lambda)$  and  $k(\lambda)$  and the film thickness can be extracted by fitting the experimental data to a parametric model of the sample. Detailed information about spectroscopic ellipsometry can be found in the text by Azzam and Bashara.<sup>18</sup> In a previous article,<sup>17</sup> we reported the results of VASE studies of the major vibrational modes of the ferroelectric copolymer Langmuir–Blodgett (LB) films in the spectral range 600–1600  $\text{cm}^{-1}$ . We also

<sup>a)</sup>Also with the Department of Physics, Ivanovo State University, Ivanovo 153025, Russia.

<sup>b)</sup>Author to whom correspondence should be addressed; electronic mail: sducharme1@unl.edu

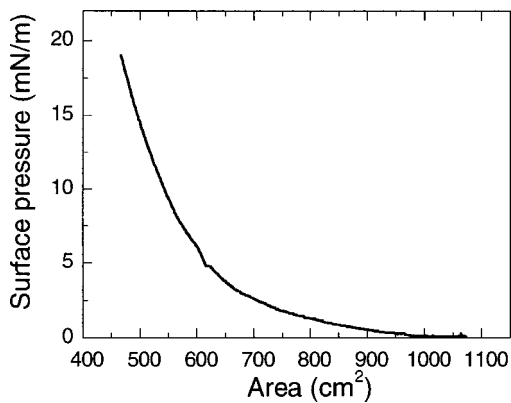


FIG. 1. The pressure-area isotherm of P(VDF/TrFE 70/30) copolymer surface layer on water subphase as the film is compressed at 25 °C.

determined the infrared absorption constants and refractive indices by analyzing the experimental data. A similar approach is used in this work to obtain the optical properties of the copolymer LB film in the visible and ultraviolet range. In addition, multi-sample analysis was used to refine the optical dispersion curve and determine the film thickness of all the samples.

## II. EXPERIMENT

The films of P(VDF/TrFE) copolymer with 70/30 molar ratio were made by the horizontal (Schaefer) variation of the Langmuir–Blodgett technique using a NIMA model 622C automated LB trough filled with ultrapure ( $>18\text{ M}\Omega\text{ cm}$ ) water. The copolymer was dissolved in dimethyl sulfoxide at 80 °C to prepare a 0.01% solution (by weight). Approximately 1 mL of the solution at room temperature was dispersed on the surface of the water, which was kept at 25 °C. The surface film was compressed slowly to a surface pressure of 5 mN/m to form a uniform layer. Figure 1 shows the typical surface pressure-area isotherm when the surface film is compressed. The expanding curve showed reversible behavior without significant area loss.<sup>19</sup> The film was transferred onto a solid substrate at constant pressure by horizontal dipping, repeating until the desired number of monolayers (ML) was deposited. The films for the VASE measurements were deposited on electronic-grade Si (100) wafers, and annealed at either 120 or 125 °C for 1 h to improve crystallinity. The copolymer LB film deposition methods are described in detail in Ref. 15.

A commercially available VASE system was used to record the ellipsometry data,  $\psi(\lambda, \theta)$  and  $\Delta(\lambda, \theta)$  at multiple incident angles ( $\theta=55^\circ$ ,  $65^\circ$  and  $75^\circ$ ) and over a wide wavelength range, from 200 to 1700 nm (0.75–6.5 eV), with a resolution of 2 nm or better. A second VASE system was used to record  $\psi(\lambda, \theta)$  and  $\Delta(\lambda, \theta)$  for incident angles  $\theta=45^\circ$ ,  $55^\circ$ ,  $65^\circ$ , and  $75^\circ$  over the wavelength range 130–1700 nm (0.75–9.5 eV), with a resolution of 0.05 eV or better. All the VASE data were recorded at room temperature.

## III. RESULTS AND DISCUSSION

The optical properties of the copolymer films were obtained from the VASE data by using a multilayer model with

adjustable parameters to represent the optical properties of the layers. The mean square difference between the experimental data and the model-generated data were minimized by adjusting the model parameters.<sup>20</sup> The optical properties of the Si substrate (with 4.3 nm native oxide in this case) were independently calibrated by the spectroscopic ellipsometry before film deposition and fixed for the sample fitting procedure to reduce the number of adjustable parameters, so only the properties of copolymer LB films were varied. In fitting the data, we further assumed that the LB film was optically uniaxial. This validity of this assumption was confirmed by the polarized infrared studies.<sup>17</sup> In the visible and ultraviolet range, the copolymer films are transparent with very low absorption.<sup>7,15</sup> Cauchy dispersion functions were used to represent both in-plane and out-of-plane optical properties of the film, each with the form  $n(\lambda) = n_0 + b/\lambda^2 + c/\lambda^4$ , and  $k(\lambda) = \alpha \exp[\beta(1/\lambda - 1/\lambda_0)]$ , where  $n_0$ ,  $b$ ,  $c$ ,  $\alpha$ ,  $\beta$ , and  $\lambda_0$ , are constants. To further reduce the correlation among the parameters in the fitting process and improve accuracy, a multi-sample data analysis technique was used.<sup>17,20–22</sup> This technique fits the VASE data  $\psi(\lambda, \theta)$  and  $\Delta(\lambda, \theta)$  for samples with the same substrate properties, but different thickness  $d$ , and assumes that the optical constants  $n(\lambda)$  and  $k(\lambda)$  are independent of thickness (and that the films are uniaxial). As will be shown below, this is a good approximation for the copolymer LB film with the thickness ranging from 5 to 125 ML.

The VASE data were recorded using two instruments, one operating from 0.75 to 6.5 eV and the other from 0.75 to 9.5 eV. The multi-sample data analysis was done independently for each instrument. VASE data recorded at incident angle  $\theta=55^\circ$ ,  $65^\circ$  and  $75^\circ$  from samples with the thickness 20, 30, 55, 65, 80, 100, and 110 ML were fit simultaneously using multi-sample analysis in the range 0.75–6.5 eV, and the model-generated data fit the experimental data very well. The 55, 65, 80, and 100 ML samples were further characterized by another VASE system in the range 0.75–9.5 eV and fit using multi-sample analysis. Again, the model-generated data fit the experimental data well in the range 0.75 to 8.0 eV as shown in Fig. 2 for the 100 ML sample recorded at incident angle  $\theta=45^\circ$ ,  $55^\circ$ ,  $65^\circ$  and  $75^\circ$ . [The value of  $\Delta(\lambda, \theta)$  is limited to the interval from  $-90^\circ$  to  $270^\circ$  and so jumps between the end points as at 2.75, 4.50, 4.71 and 7.14 eV for  $\theta=75^\circ$  in Fig. 2(b)]. The same model fit the data from the other three samples equally well. The fit is less accurate in the region of strong band gap absorption around 7–8 eV,<sup>12</sup> where the Cauchy approximation is not adequate. The film optical properties obtained from the two instruments agreed within 0.5% over the range of overlap. The differences in film thickness obtained from both fitting processes for the 55, 65, 80, and 100 ML samples are all less than 1%. However, we cannot tell whether these small differences are due to the variation in film thickness or the differences in calibration between the two VASE systems.

Figure 3 shows the optical refractive indices  $n_{\parallel}$  and  $n_{\perp}$  over the range 155–1700 nm, obtained from the VASE multi-sample analysis, plus the data from the infrared range 1.7–35  $\mu\text{m}$  reported in a previous article.<sup>17</sup> Table I summarizes the present values of the optical refractive indices at

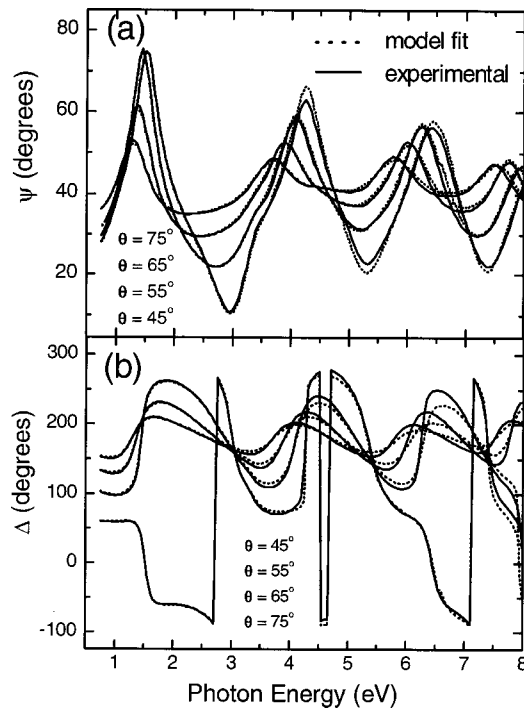


FIG. 2. Ellipsometry measurements of  $\psi$  and  $\Delta$  (solid lines) from a 100 ML copolymer LB film for angles of incidence  $\theta=45^\circ$ ,  $55^\circ$ ,  $65^\circ$ , and  $75^\circ$  and the Cauchy model fits (dotted lines) in the spectral range 0.75–8.0 eV obtained from the VASE multi-sample analysis.

two wavelengths with values reported in the literature for spin-coated films<sup>7,8</sup> and highly oriented “single crystal-like films.”<sup>9</sup> We calculated the expected values of  $n_{\parallel}$  and  $n_{\perp}$  from the literature data by assuming that the LB films had uniform (110) crystal orientation perpendicular to the film, but are rotationally averaged in the film plane (hence the uniaxial model). The refractive indices calculated from measurements on the spin-coated films<sup>7,8</sup> and highly oriented single crystal-like films,<sup>9</sup> reported in the literature are also shown in Fig. 3 for comparison. The attenuation constants  $k_{\parallel}$

TABLE I. List of the refractive indices  $n_a$ ,  $n_b$  and  $n_c$  (along the crystal main axes  $a$ ,  $b$  and  $c$ ), and the values of  $n_{\parallel}$  and  $n_{\perp}$  (perpendicular and parallel to the film plane) for (110)-oriented uniaxial films of PVDF/TrFE copolymers.

| $n_a$              | $n_b$              | $n_c$              | $n_{\perp}$        | $n_{\parallel}$    | Wavelength (nm) |
|--------------------|--------------------|--------------------|--------------------|--------------------|-----------------|
|                    |                    |                    | 1.412 <sup>a</sup> | 1.420 <sup>a</sup> | 633             |
| 1.404 <sup>b</sup> | 1.438 <sup>b</sup> | 1.540 <sup>b</sup> | 1.429 <sup>b</sup> | 1.474 <sup>b</sup> | 633             |
|                    |                    |                    | 1.408 <sup>c</sup> | 1.432 <sup>c</sup> | 633             |
| 1.397 <sup>d</sup> | 1.397 <sup>d</sup> | 1.440 <sup>d</sup> | 1.397 <sup>d</sup> | 1.418 <sup>d</sup> | 514             |
|                    |                    |                    | 1.410 <sup>c</sup> | 1.436 <sup>c</sup> | 514             |

<sup>a</sup>From Ref. 7, which used the Brewster angle method on 70/30 copolymer.

<sup>b</sup>From Ref. 9, which used the Brewster angle method on 71/29 copolymer. The values of  $n_{\perp}$  and  $n_{\parallel}$  were calculated from the  $n_a$  and  $n_b$  values for a random crystal orientation model with the (110) plane along the normal direction ( $n_{\perp}$ ).

<sup>c</sup>From this work, using spectroscopic ellipsometry on 70/30 copolymer LB films.

<sup>d</sup>From Ref. 8, which used an Abbe refractometer method on 70/30 copolymer. The values of  $n_{\perp}$  and  $n_{\parallel}$  were calculated from the  $n_a$  and  $n_b$  values for a random crystal orientation model with the (110) plane along the normal direction ( $n_{\perp}$ ).

and  $k_{\perp}$  obtained from the multi-sample analysis are shown in Fig. 4. They are very small over the entire range, but increase with energy due to electronic excitations near the band gap.<sup>12,16</sup>

The optical dispersion data shown in Figs. 3 and 4 has the following features: both in-plane and out-of-plane optical properties satisfy the Cauchy dispersion form, except in the spectral ranges 6.8–11.8  $\mu\text{m}$  where there are strong molecular vibrational modes.<sup>23</sup> (Note that the birefringence  $n_{\parallel} - n_{\perp}$  changes sign across the vibrational bands, due to the difference between vibrational and electronic mode symmetries.)

In order to better understand the optical dispersion and to check the self-consistency of the results, we compared the data for  $\psi(\lambda, \theta)$  and  $\Delta(\lambda, \theta)$  in the range 0.035–3.0 eV from the 100 ML sample of the present study with the results of a Lorentz oscillator model fit, determined previously from IR-VASE measurements of similar LB films of the same

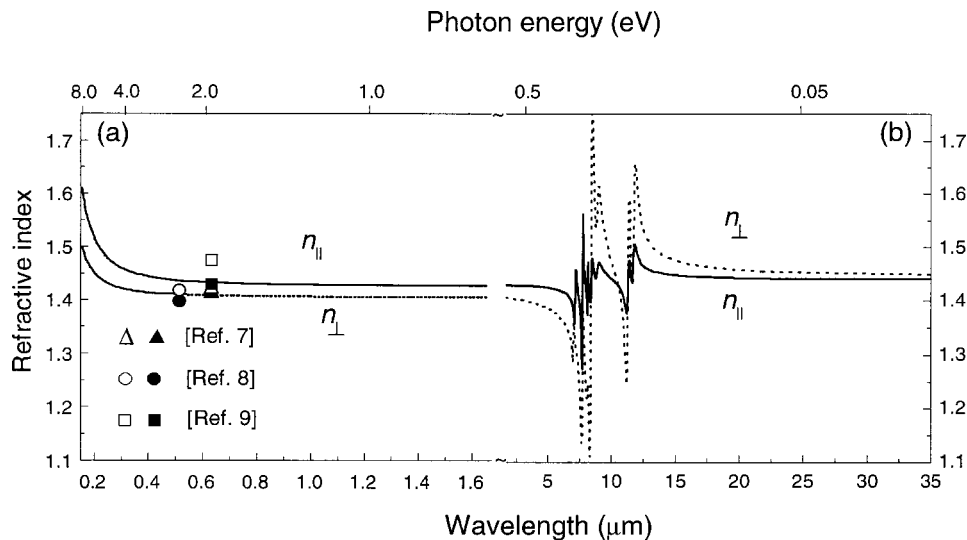


FIG. 3. The refractive indices for in-plane  $n_{\parallel}$  (solid line) and out-of-plane  $n_{\perp}$  (dashed line) polarization, obtained from the VASE multi-sample data analysis in the spectral range 0.155 to 35  $\mu\text{m}$ . The open symbols are for the in-plane refractive index and solid ones for the out-of-plane refractive index.

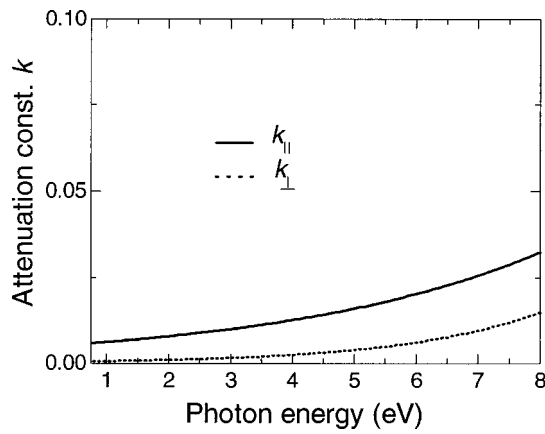


FIG. 4. The attenuation constants for in-plane  $k_{||}$  (solid lines) and out-of-plane  $k_{\perp}$  (dashed line) polarization, obtained from the VASE multi-sample analysis in the spectral range 0.75–8.0 eV.

composition.<sup>17</sup> The model calculations are in excellent agreement with the experimental data, as shown in Fig. 5.

The thickness of each film was also extracted from the VASE multi-sample analysis using the common optical dispersion curve (Fig. 3) and these values are plotted in Fig. 6(a) as circles. The same optical dispersion was used to determine the thickness of several other LB films of the same copolymer, deposited on Si substrates and annealed at 125 °C. The thicknesses of 5, 50, and 90 ML films are shown as squares in Fig. 6(a). A series of LB films was fabricated on a single 3 in Si wafer by depositing a few layers, wiping off part of the wafer, and repeating, to make films in a pie-shaped pattern [see the inset to Fig. 6(a)], and the thicknesses

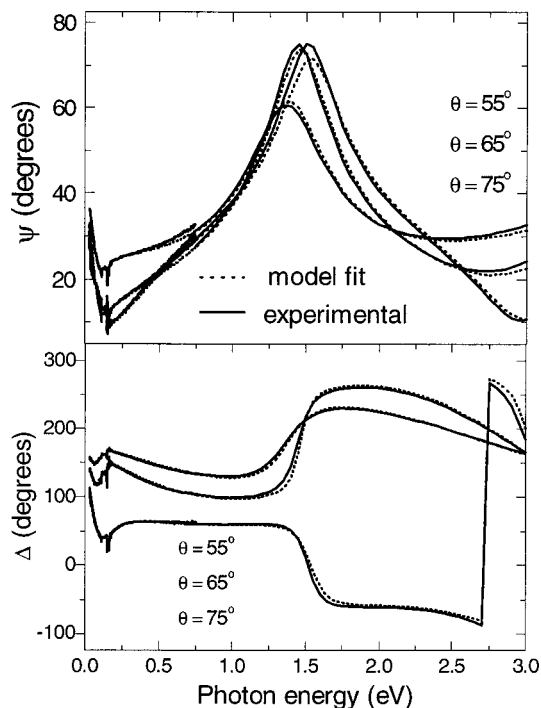


FIG. 5. Ellipsometry measurements of  $\psi$  and  $\Delta$  (solid lines) from a 100 ML copolymer LB film for angles of incidence  $\theta=55^\circ$ ,  $65^\circ$ , and  $75^\circ$  in the spectral range 0.035–3.0 eV and the expected results from the Lorentz oscillator model (dotted lines).

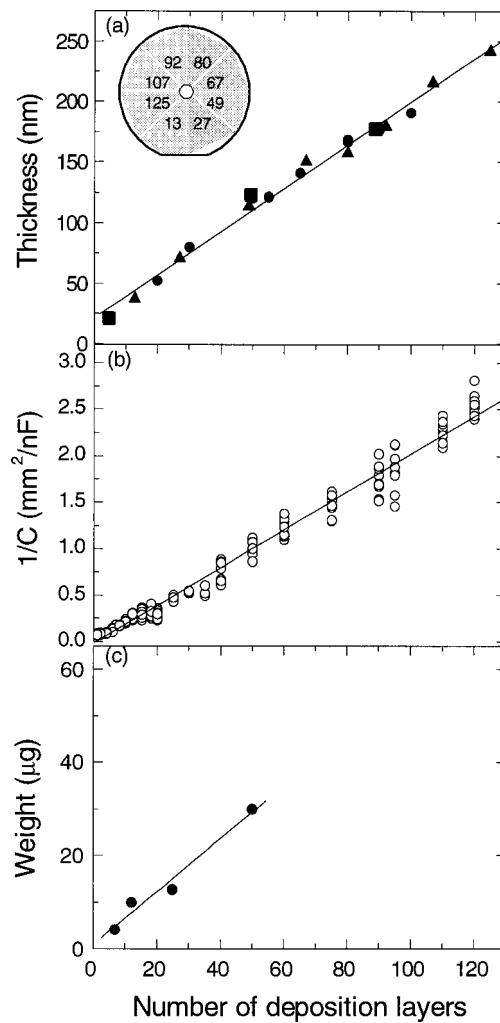


FIG. 6. (a) The thickness of several sets of LB films: the set used for VASE multi-sample analysis (circles); LB films of 5, 50, and 90 ML (squares); the sections of the pie-shaped sample shown in the inset (triangles). (b) The specific capacitance of a series of LB film capacitors. (c) The mass of LB films deposited on quartz microbalance substrates. The solid lines in each graph are linear regression fits to the data.

indicated by triangles in Fig. 6(a). The plot in Fig. 6(a) has a slope of  $1.78 \pm 0.07$  nm/ML, representing the average thickness per nominal monolayer. There is a small deviation for the two thinnest films, suggesting that initial layers, and films of about 20 ML or less, may be thinner on average.

With the film thickness calibrated, one can determine the dielectric constant perpendicular to the film by measuring the capacitance. For this study, we made a separate set of LB films from 1 to 120 ML in thickness. Each sample was made by first evaporating a series of parallel aluminum stripes 1–3 mm wide and 100 nm thick on a glass slide, depositing the copolymer LB film, and then evaporating an identical set of aluminum electrodes at right angles to the first set. This resulted in samples with 4–6 independent capacitors. The capacitance of each was measured at 1 kHz with 0.1 V amplitude using a Hewlett-Packard 4192A impedance analyzer. The

results of these measurements are shown in Fig. 6(b), exhibiting excellent linearity with slope  $0.0203 \pm 0.0004$  mm<sup>2</sup>/nF/ML over the entire thickness range, and

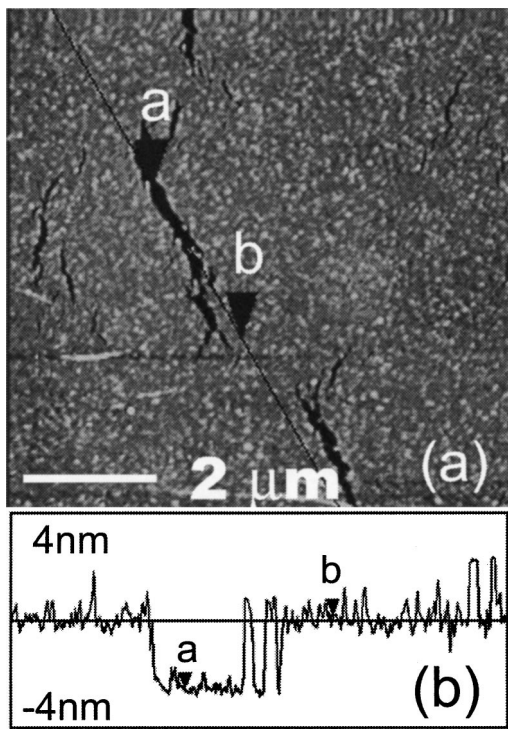


FIG. 7. Atomic force microscopy image of a 1 ML sample deposited on a Si<sub>3</sub>N<sub>4</sub> substrate (b) The AFM image profile along the line in (a). The arrow positions at *a* and *b* in (b) correspond to the arrow positions in (a).

with negligible offset. Combining this slope with the thickness calibration from ellipsometry, we find that the perpendicular dielectric constant of the copolymer LB films is  $9.9 \pm 0.4$ , in excellent agreement with values reported elsewhere for the 70/30 copolymer.<sup>13,14</sup>

Another technique used to determine film thickness consisted of depositing films in a quartz microbalance method and measuring the frequency shift and other oscillator parameters to measure film mass.<sup>24</sup> Identical quartz crystals (300 kHz resonant frequency) supporting contour shear oscillations were used. A self-balancing bridge with frequency multiplier was used to measure equivalent electric parameters (capacitance, inductance, active resistance) of the oscillator. After a calibration of four bare crystals, each with total surface area  $1.89 \pm 0.03 \text{ cm}^2$ , they were covered on both sides by 7, 12, 25, and 50 ML copolymer films. The oscillator resonance data, along with the known crystal inductance and geometry were used to calculate the weight of the films by algorithms described elsewhere.<sup>25,26</sup> Figure 6(c) shows the dependence of film weight on the number of layers, yielding a slope of  $0.59 \pm 0.03 \text{ mg/ML}$ . Dividing this mass by the crystal area and transfer rate yields the film density of  $1.75 \pm 0.12 \text{ g/cm}^3$ , in excellent agreement with the values  $1.79\text{--}1.89 \text{ g/cm}^3$  reported for the 70/30 copolymers,<sup>13,14,27</sup> and the value  $1.786 \text{ g/cm}^3$  obtained from the unit cell measured by neutron powder diffraction.<sup>27</sup>

The thickness of a 1 ML film deposited on Si, but not annealed, was also measured by atomic force microscopy (AFM). During the deposition, the continuous surface film sometimes cracks, leaving small gaps, as shown in Fig. 7(a). The AFM image profile shown in Fig. 7(b) gives the film

thickness of  $2.2 \pm 0.2 \text{ nm}$ , by assuming the flat-bottomed region in Fig. 7(b) represents the total absence of the film. Additional AFM measurements show that the 1 ML fresh film thickness is in the range 1.4–2.2 nm, depending slightly on the deposition surface pressure.

The above measurements show that the average thickness of a single deposited layer is  $1.78 \pm 0.07 \text{ nm}$ , greater than the expected value of 0.45 nm for the interlayer spacing along the (110) crystal orientation (approximately equal to the polymer chain diameter) as measured by the x-ray diffraction from the copolymer LB films.<sup>15</sup> Furthermore, the measurements of capacitance and weight are consistent with this transfer rate. This indicates that the structure of the film on the trough is more complex than an ideal monomolecular layer,<sup>28</sup> possibly due to stacking and folding of the polymer chains.

#### IV. CONCLUSIONS

The optical dispersion of ferroelectric P(VDF/TrFE 70/30) copolymer LB films was measured over the entire range from infrared (0.035 eV) to ultraviolet (8 eV) using variable-angle spectroscopic ellipsometry. The spectra are consistent with optically uniaxial films with optical constants that are independent of thickness. The film thickness determined by multi-sample analysis gives a deposition rate of  $1.78 \pm 0.07 \text{ nm}$  per deposition layer. This, in turn, was used to calibrate a series of capacitance measurements to determine the dielectric constant of  $9.9 \pm 0.4$ , also without significant dependence on film thickness.

#### ACKNOWLEDGMENTS

The authors thank Li Yan from the Department of Electrical Engineering for her kind assistance with the VASE systems. This work was supported by the National Science Foundation Small-Business Innovation Research Program (DMI-9901510, ECS-0070245), the Office of Naval Research, and the Nebraska Research Initiative.

<sup>1</sup>The Applications of Ferroelectric Polymers, edited by T. T. Wang, J. M. Herbert, and A. M. Glass (Chapman and Hall, New York, 1988).

<sup>2</sup>R. G. Kepler, in *Ferroelectric Polymers*, edited by H. S. Nalwa (Dekker, New York, 1995), p. 183.

<sup>3</sup>J. G. Bergman, J. H. McFee, and G. R. Crane, *Appl. Phys. Lett.* **18**, 203 (1971).

<sup>4</sup>M. H. Berry and D. N. Gookin, in *Proceedings of the Conference on Nonlinear Optical Properties of Organic Materials*, San Diego, 17–19 August, edited by G. Khanarian (SPIE, Bellingham, WA, 1988), Vol. 971, p. 154.

<sup>5</sup>D. Broussoux and F. Micheron, *J. Appl. Phys.* **51**, 2020 (1980).

<sup>6</sup>D. K. Das-Gupta, K. Doughty, and D. B. Shier, *J. Electrostat.* **7**, 267 (1979).

<sup>7</sup>B. Berge, A. Wicker, J. Lajzerowicz, and J. F. Legrand, *Europhys. Lett.* **9**, 657 (1989).

<sup>8</sup>J. K. Krüger, B. Heydt, C. Fischer, J. Baller, R. Jiménez, K.-P. Bohn, B. Servet, P. Galtier, M. Pavel, B. Ploss, M. Beghi, and C. Bottani, *Phys. Rev. B* **55**, 3497 (1997).

<sup>9</sup>Y. Tajitsu, K. Kado, K. Okubo, and H. Ohigashi, *J. Mater. Sci. Lett.* **19**, 295 (2000).

<sup>10</sup>M. Cakmak and Y. Wang, *J. Appl. Polym. Sci.* **37**, 977 (1989).

<sup>11</sup>K. S. Spector and R. S. Stein, *Macromolecules* **24**, 2083 (1991).

<sup>12</sup>C. Duan, W. N. Mei, J. R. Hardy, S. Ducharme, J. Choi, and P. A. Dowben, *Europhys. Lett.* **61**, 81 (2003).

<sup>13</sup>T. Furukawa, *Phase Transitions* **18**, 143 (1989).

<sup>14</sup>K. Omote, H. Ohigashi, and K. Koga, *J. Appl. Phys.* **81**, 2760 (1997).

- <sup>15</sup>S. Ducharme, S. P. Palto, and V. M. Fridkin, in *Handbook of Thin Film Materials*, edited by H. S. Nalwa (Academic, New York, 2002), Vol. 3, p. 545.
- <sup>16</sup>J. Choi, P. A. Dowben, S. Pebley, A. V. Bune, S. Ducharme, V. M. Fridkin, S. P. Palto, and N. Petukhova, *Phys. Rev. Lett.* **80**, 1328 (1998).
- <sup>17</sup>M. Bai, M. Poulsen, A. V. Sorokin, S. Ducharme, C. M. Herzinger, and V. M. Fridkin, *J. Appl. Phys.* **94**, 195 (2003).
- <sup>18</sup>R. M. A. Azzam and N. M. Bashara, *Ellipsometry and Polarized Light* (North-Holland, Amsterdam, 1977).
- <sup>19</sup>S. Palto, L. Blinov, A. Bune, E. Dubovik, V. Fridkin, N. Petukhova, K. Verkhovskaya, and S. Yudin, *Ferroelectr., Lett. Sect.* **19**, 65 (1995).
- <sup>20</sup>C. M. Herzinger, H. Yao, P. G. Snyder, F. G. Celii, Y. C. Kao, B. Johs, and J. A. Woollam, *J. Appl. Phys.* **77**, 4677 (1995).
- <sup>21</sup>B. Li, T. He, M. Ding, P. Zhang, F. Gao, and F. Jing, *J. Mater. Res.* **13**, 1368 (1998).
- <sup>22</sup>M. I. Sluch, C. Pearson, M. C. Petty, M. Halim, and I. D. W. Samuel, *Synth. Met.* **94**, 285 (1998).
- <sup>23</sup>K. Tashiro, in *Ferroelectric Polymers*, edited by H. S. Nalwa (Dekker, New York, 1995), p. 63.
- <sup>24</sup>*Application of Piezoelectric Quartz Crystal Microbalances*, edited by C. Lu and A. W. Czanderna (Elsevier, New York, 1984).
- <sup>25</sup>V. E. Savchenko, *J. Eng. Phys. Thermophys.* **43**, 784 (1982).
- <sup>26</sup>V. E. Savchenko, *J. Eng. Phys. Thermophys.* **70**, 169 (1997).
- <sup>27</sup>E. Bellet-Amalric and J. F. Legrand, *Eur. Phys. J. B* **3**, 225 (1998).
- <sup>28</sup>A. V. Bune, V. M. Fridkin, S. Ducharme, L. M. Blinov, S. P. Palto, A. V. Sorokin, S. G. Yudin, and A. Zlatkin, *Nature (London)* **391**, 874 (1998).